Electronic Supplementary Material (ESI) for Inorganic Chemistry Frontiers.

Solid polymorphism and dynamic magnetic properties of dodecylated vanadyl-porphyrinato complex: Spin-lattice relaxations suppressed by phase stabilization

Yoji Horii,*[a] Momo Makino,[a] Taro Yamamoto,[b] Shoichi Tatsumi,[b] Hal Suzuki,[b] Mariko Noguchi,[c] Takefumi Yoshida,[d] Takashi Kajiwara,[a] Zhao-Yang Li[e] and Masahiro Yamashita*[e,f]

[a] *Department of Chemistry, Faculty of Science, Nara Women's University, Nara 6308506, Japan.*

[b] *Department of Chemistry, Kindai University, 3-4-1 Kowakae, Higashiosaka, Osaka 577-8502, Japan.*

[c] *Graduate School of Integrated Basic Sciences, Nihon University, 3-25-40 Sakurajosui, Setagaya-ku, Tokyo 156-8550, Japan*

[d] *Innovation Research Center for Fuel Cells, The University of Electro-Communications, Chofu, Tokyo 182-8585, Japan.*

[e] *School of Materials Science and Engineering, Nankai University, Tianjin 300350, China.*

[f] *Department of Chemistry, Graduate School of Science, Tohoku University 6-3 Aramaki-Aza-Aoba Aoba-ku, Sendai, Miyagi, 980-8578, Japan.*

Comparison between the $\Delta_{trs}S$ value obtained by C_p measurements and that estimated by SCXRD analyses.

SCXRD analyses for **1m** at 153 K revealed that there are at least three confirmations on alkyl chains. Taking into account the VO-up and VO-down conformations, W value of **1m** is 3 × 3 × 2 = 18 at 153 K. At 283 K, one dodecyl chain of **1m** showed at least 8 conformations. Therefore, the W value of **1** at 283 K is expected to be 8 × 8 × 2 = 128. Then, the ratio between W values at 283 K and 153 K ($W_{283\ K}W_{153\ K}^{-1}$) is estimated to be 7.1. This value is lower than the ratio of W at high (W_{HT}) and low (W_{LT}) temperature determined by ΔS value of the broad C_p peak, that is $W_{HT}W_{LT}^{-1} = \exp(20.3/R) = 11.5$, where R is the gas constant.

According to the SCXRD analyses for **1s**, W value at 153 K and 200 K were 2 × 2 × 2 = 8 and 4 × 4 × 2 × 2 × 2 = 128, respectively. At 283 K, only eight kinds of conformation were visible due to heavy disorders on dodecyl chains. Therefore, the ratio of the number of conformations obtained by SCXRD is $W_{200\ K}W_{153\ K}^{-1} = 16$ at most. This value is much lower than the ratio of W at high (W_{HT}) and low (W_{LT}) temperature determined by ΔS value of the broad C_p peak, that is $W_{HT}W_{LT}^{-1} = \exp(47.9/R) = 318$, where R is the gas constant.

In both crystalline phases, the changes in W upon phase transition are smaller than those expected from $\Delta_{trs}S$ values obtained by C_p analyses, indicating the significant vibrational contribution to the S.

Table S1. Crystalline parameters for 1m and 1s.

	1m		**1s**		
T / K	153	283	153	200	283
Formula	$C_{48}H_{62}N_2O_{4.5}V_{0.5}$		$C_{48}H_{62}N_2O_{4.5}V_{0.5}$		
Crystal system	Monoclinic		Monoclinic		
Space group	$P2_1/n$		$C2/c$		
Z	4		8		
a / Å	15.6779(6)	16.4545(13)	34.152(3)	47.983(15)	47.906(15)
b / Å	10.8485(3)	10.8002(6)	10.8810(4)	10.7204(7)	10.8092(7)
c / Å	26.9794(11)	26.018(3)	27.732(2)	27.092(2)	27.354(8)
α / °	90	90	90	90	90
β / °	104.186(4)	103.803(10)	124.983(12)	141.08(6)	140.90(6)
γ / °	90	90	90	90	90
V / Å^3	4448.8(3)	4490.2(7)	8443.3(15)	8754(8)	8933(9)
ρ / g cm^{-3}	1.141	1.131	1.203	1.160	1.137
GOF	1.395	1.044	1.164	1.020	1.015
R_1	0.1096	0.1104	0.0790	0.0940	0.1117
wR_2	0.3282	0.2918	0.1457	0.1935	0.2700

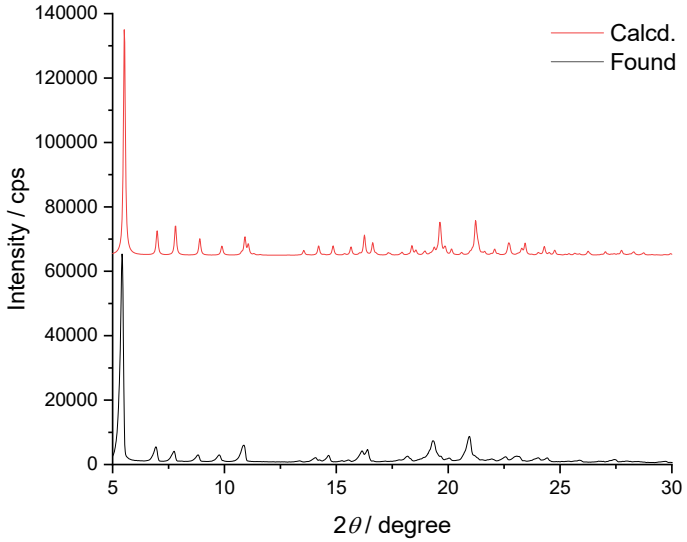

Figure S1. Experimental and calculated PXRD patterns for **1m**.

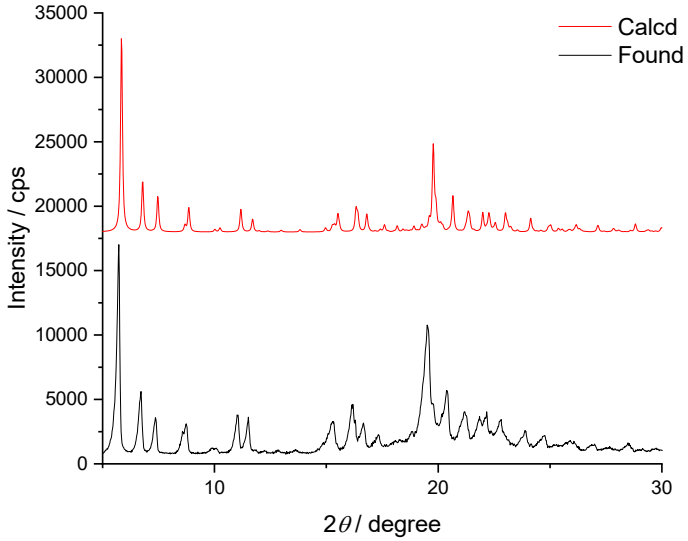

Figure S2. Experimental and calculated PXRD patterns for **1s**.

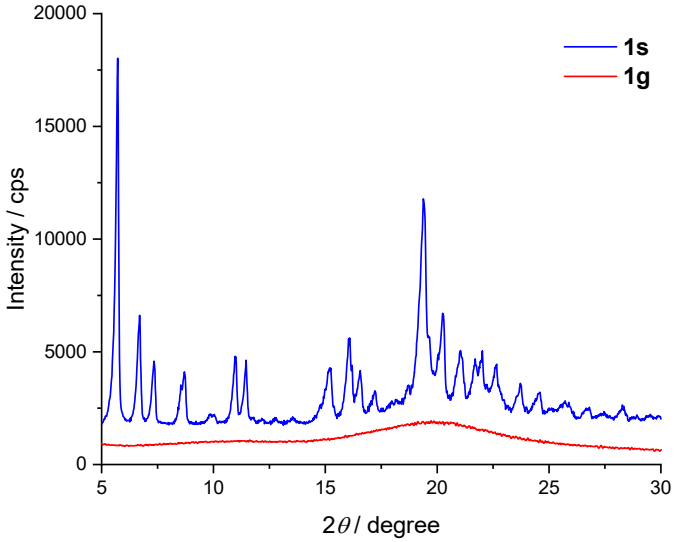

Figure S3. Comparison of PXRD patterns for **1g** and **1s**. **1g** for PXRD measurement was prepared by cooling the liquid phase using fridge. The sample cell for PXRD measurement was attached to a freezer pack to keep the temperature of **1g** at ca. 273 K. No obvious diffraction peak was observed for **1g**.

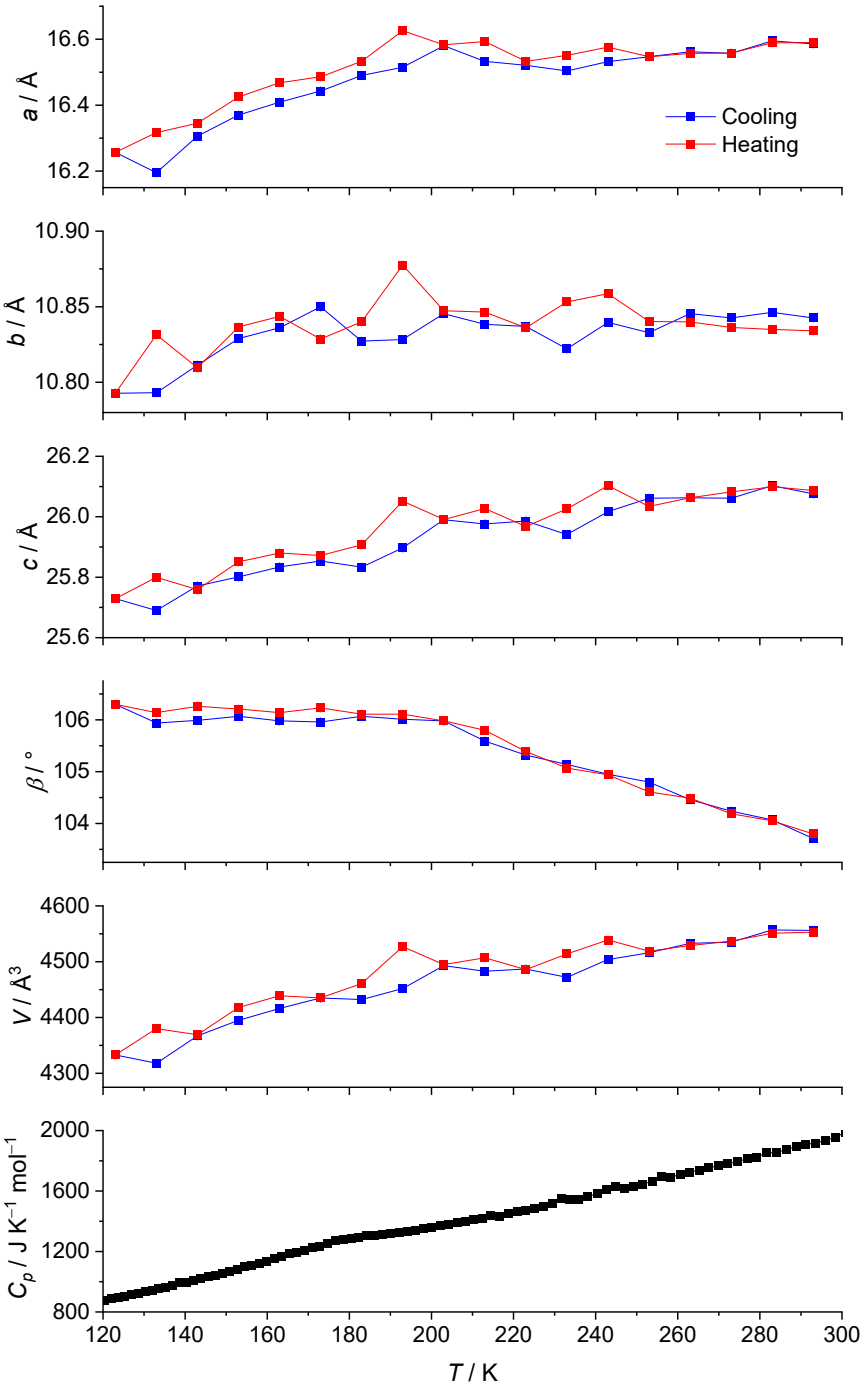

Figure S4. *T*-dependence of the crystalline parameters for single-crystal of **1m**. C_p data was shown for comparison. There is no clear anomaly in the cell parameters.

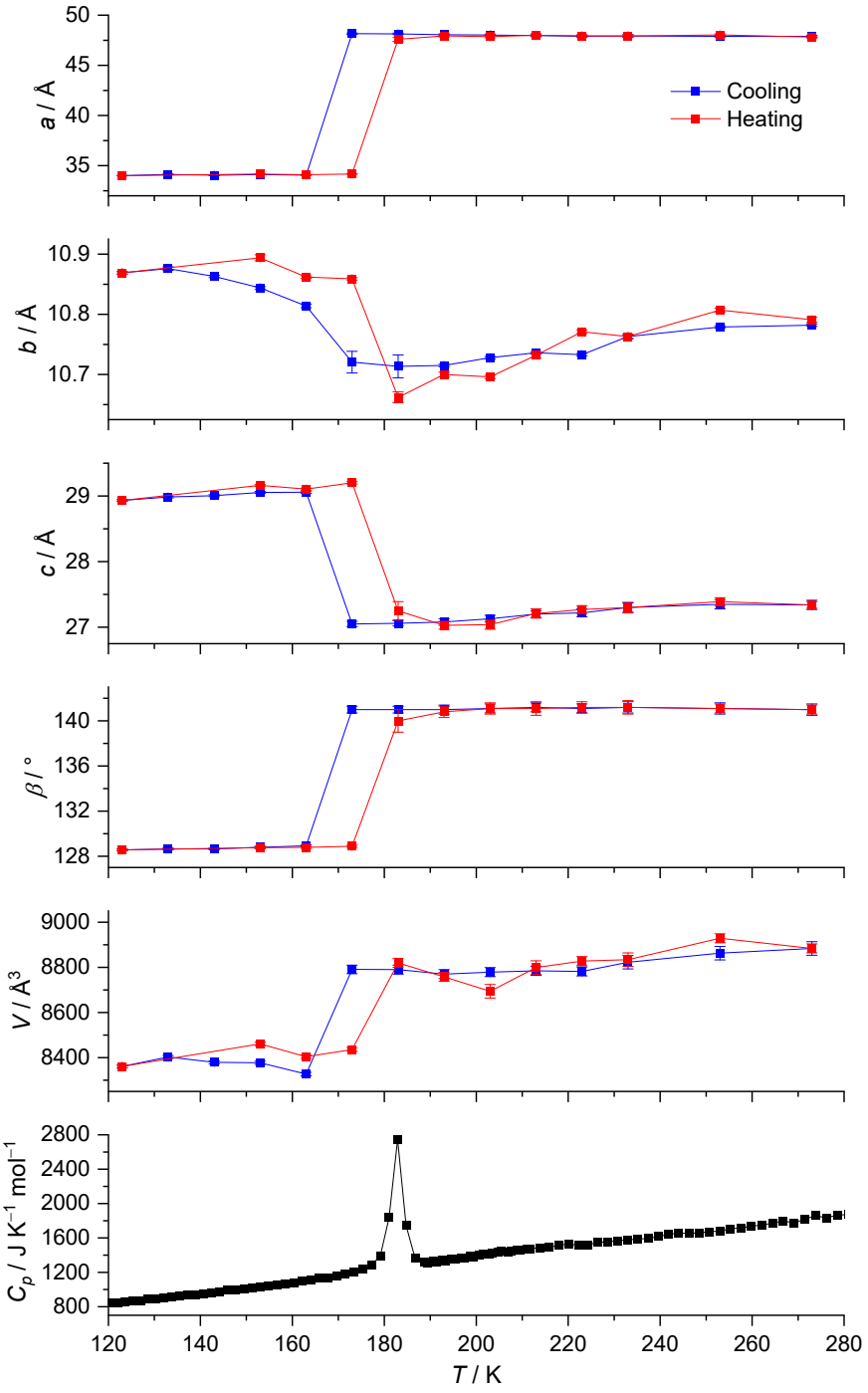

Figure S5. *T*-dependence of the crystalline parameters for single-crystal of **1s**. C_p data was shown for comparison. Sudden changes in the cell parameters are seen at around 170 K during cooling process and at around 180 K during heating process, which is attributable to the structural phase transition at 181.8 K determined by the C_p measurement.

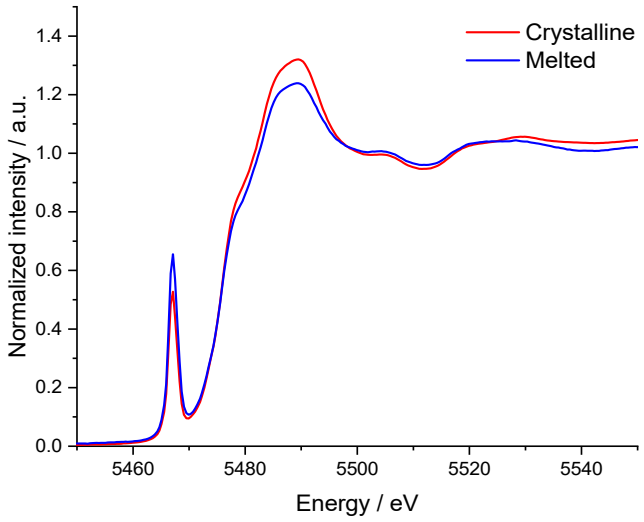

Figure S6. XAFS spectra at V *K*-edge of both crystalline and melted **1m**.

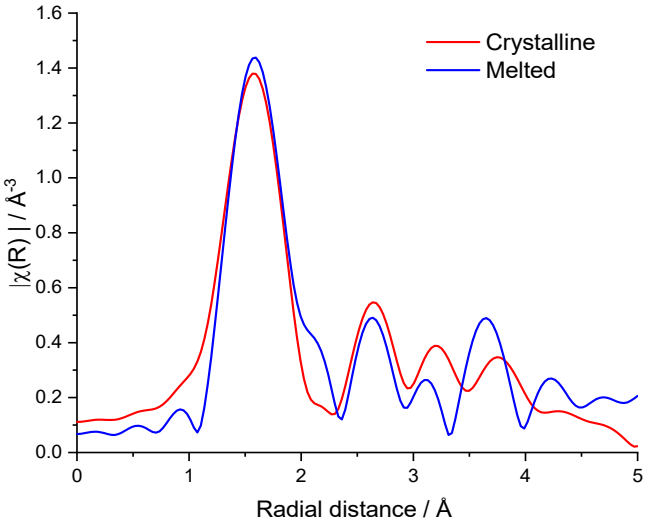

Figure S7. The Fourier transform of EXAFS at V *K*-edge of **1m** and melted sample**.** V *K*-edge of both **1m** and melted sample exhibited identical structure (especially on first sphere), indicating that coordination environment around was kept upon melting.

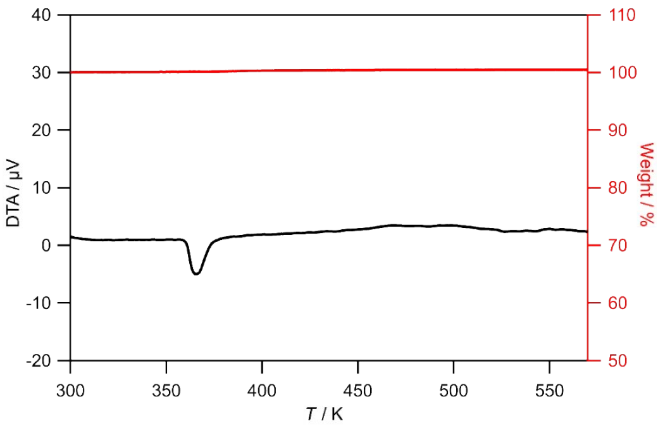

Figure S8. TG-DTA data for **1m**. Upon heating to 573 K, no significant change in weight was observed. In the DTA curve, an endothermic peak around 360 K was observed. These behaviours indicate that **1m** is sufficiently stable in the measured *T* range and that melts around 360 K.

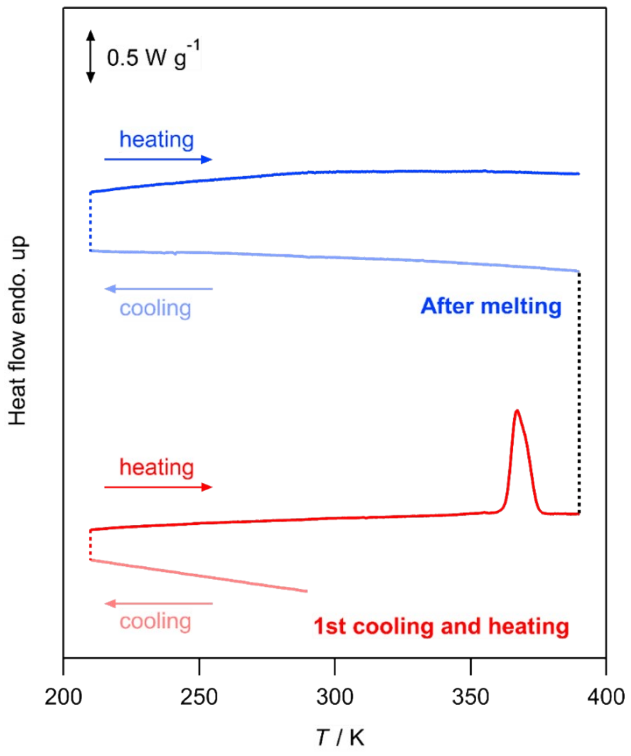

Figure S9. DSC curves for **1m** before and after melting at the heating and cooling rate of 10 K min^{-1}. No thermal anomaly was observed during the 1st cooling of **1m** from 298 K to 203 K. Upon heating (1st heating), a large endothermic peak ($\Delta_{trs}H$ = 63.1 kJ mol^{-1}) was observed at 364 K. This corresponds to the melting of **1m**, which is consistent with the DTA results (Fig. S5) and heat capacity data (Table S2). After melting, no crystallization or melting was found, and instead a glass transition was observed around 270 K. These results indicate that the glassy state (**1g**) was formed by cooling at 10 K min^{-1} after melting of **1m**.

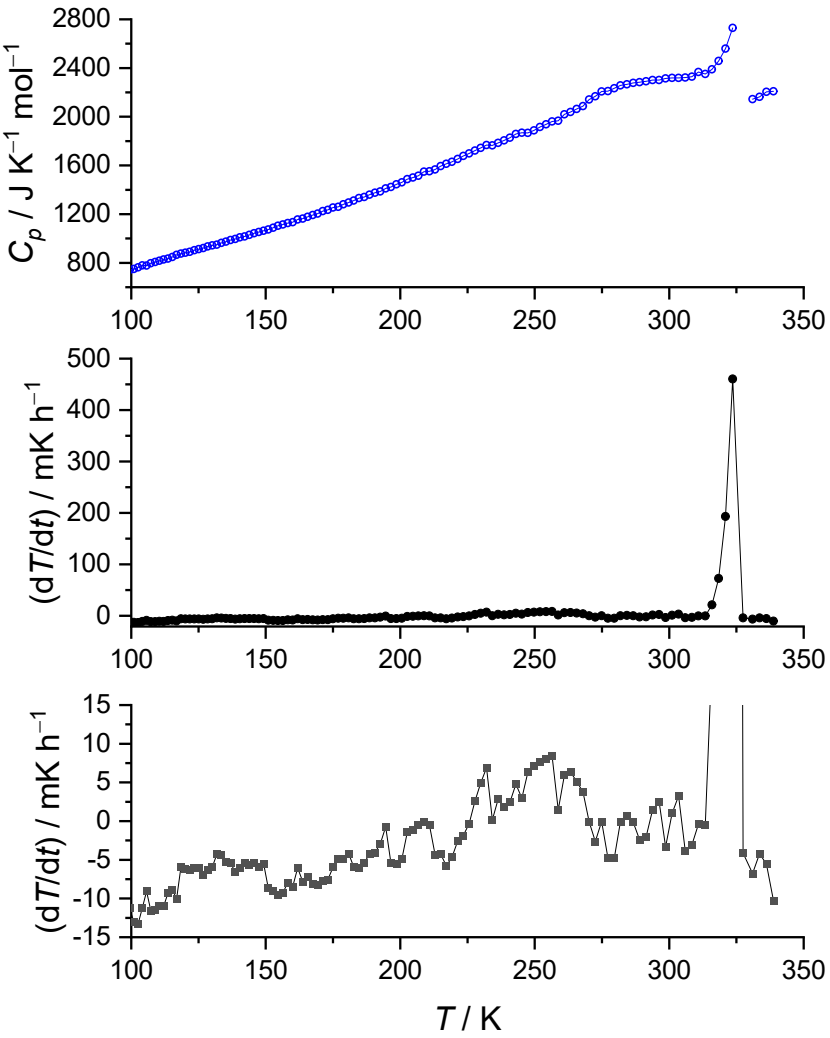

Figure S10. Crystallization of **1g** upon annealing. Sudden increase of *T*-drift (d*T*/d*t*) at *ca*. 320 K corresponds to the crystallization to **1s**. The bottom figure is the enlarged view of *T*-drift.

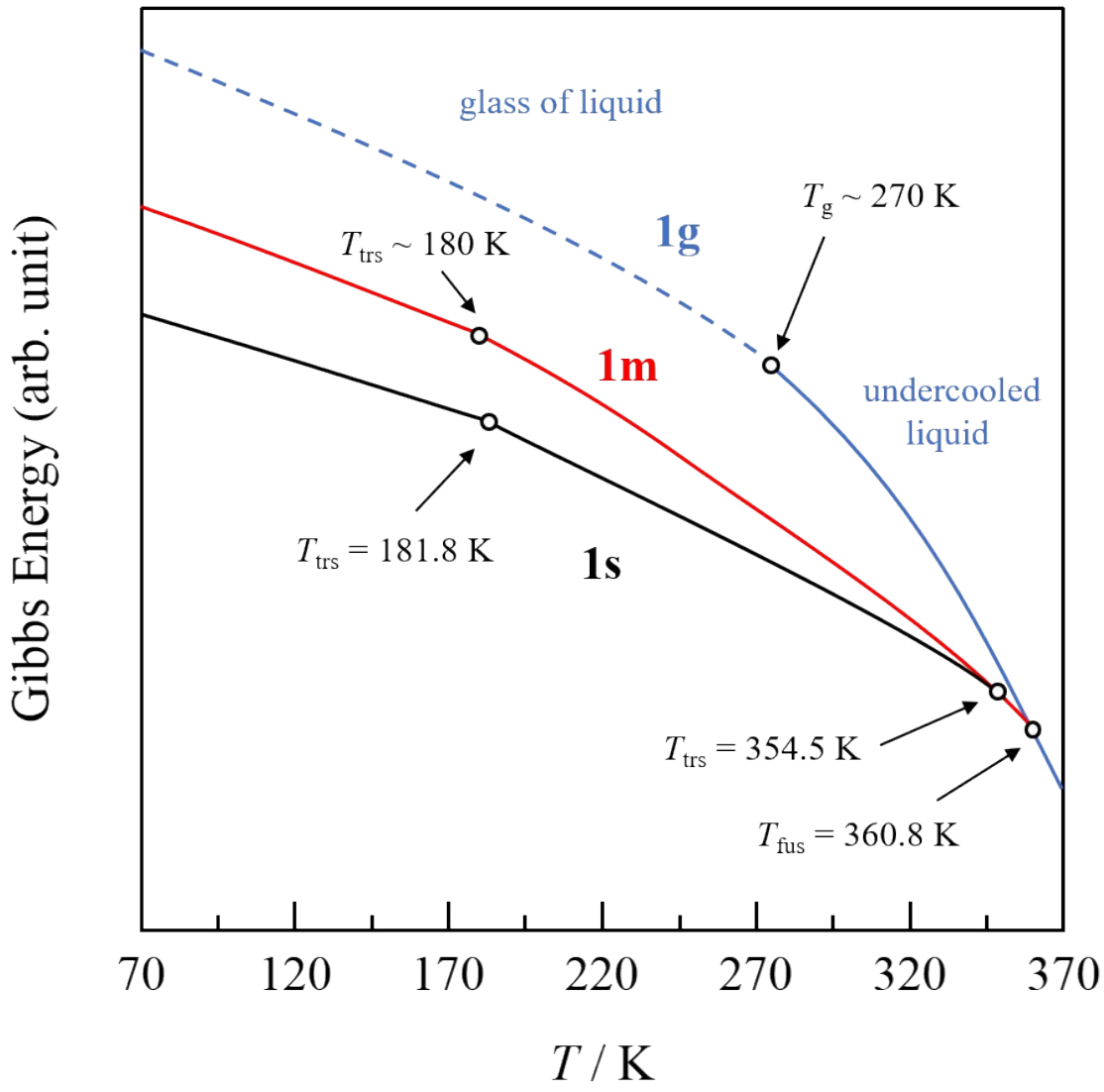

Figure S11. Schematic diagram of Gibbs energy against *T* eventually obtained for **1**.

Table S2. Summary of thermodynamic quantities of thermal anomalies.

Phase	Anomaly	Thermodynamic quantities
Liquid (**1g**)	Glass transition	$T_g \sim 270$ K
Crystal (**1m**)	Phase transition	$T_{trs} \sim 180$ K $\Delta_{trs}H = 3.47$ kJ mol^{-1} $\Delta_{trs}S = 20.3$ J K^{-1} mol^{-1}
	Fusion	$T_{fus} = 360.8$ K $\Delta_{fus}H = 55.73$ kJ mol^{-1} $\Delta_{fus}S = 154.5$ J K^{-1} mol^{-1}
Crystal (**1s**)	Phase transition	$T_{trs} = 181.8$ K $\Delta_{trs}H = 9.02$ kJ mol^{-1} $\Delta_{trs}S = 47.9$ J K^{-1} mol^{-1}
	Phase transition (**1s** → **1m**)	$T_{trs} = 354.4$ K $\Delta_{trs}H = 6.98$ kJ mol^{-1} $\Delta_{trs}S = 21.2$ J K^{-1} mol^{-1}

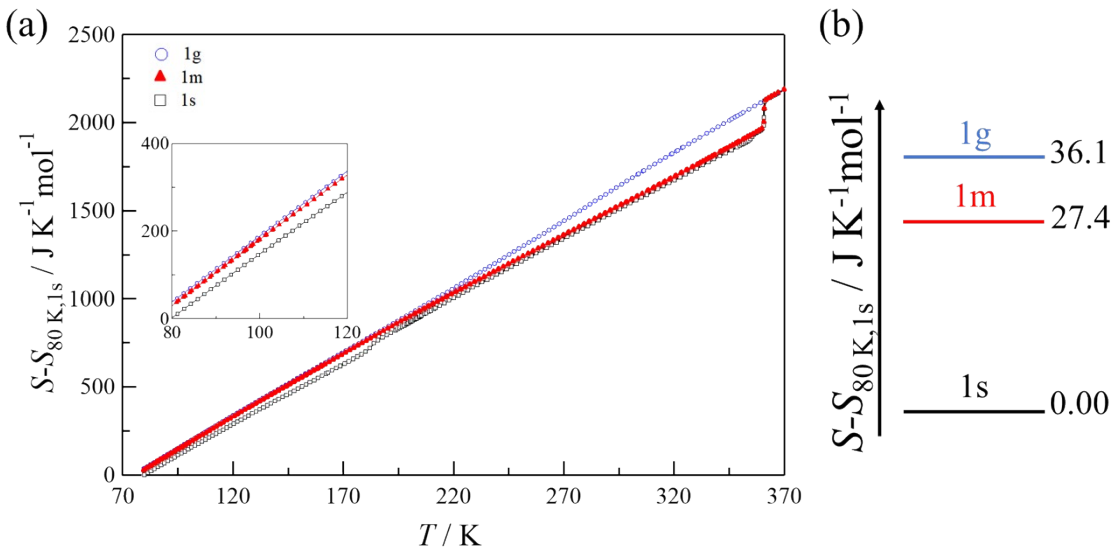

Figure S12. (a) T dependences of the entropy with respect to the entropy of **1s** at 80 K. The normal heat capacity divided by temperature C_pT^{-1} was integrated over the temperature range of 370 K to 80 K to get the entropy. After adding the contribution of the transition entropy, the curves were offset as the plots above 360.8 K (liquid phase) were superimposed, and then the point of **1s** at 80 K was set to the origin. (b) Entropy differences between **1g**, **1m** and **1s** at 80 K.

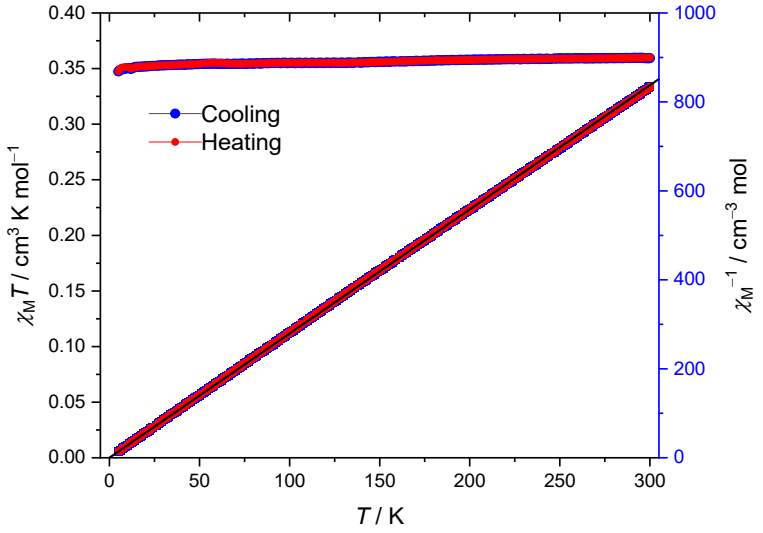

Figure S13. $\chi_M T$ vs. T plots for **1s** at a dc magnetic field of 10 kOe. No clear anomaly was found at 180 K during heating and cooling processes, indicating that the phase transitions observed in C_p measurements is attributable to the structural phase transition rather than magnetic transition. Solid line of χ_M^{-1} vs. T plots represent a fit in the T range of 20-300 K using Curie's law with the C value of 0.36 cm^3 K mol^{-1}.

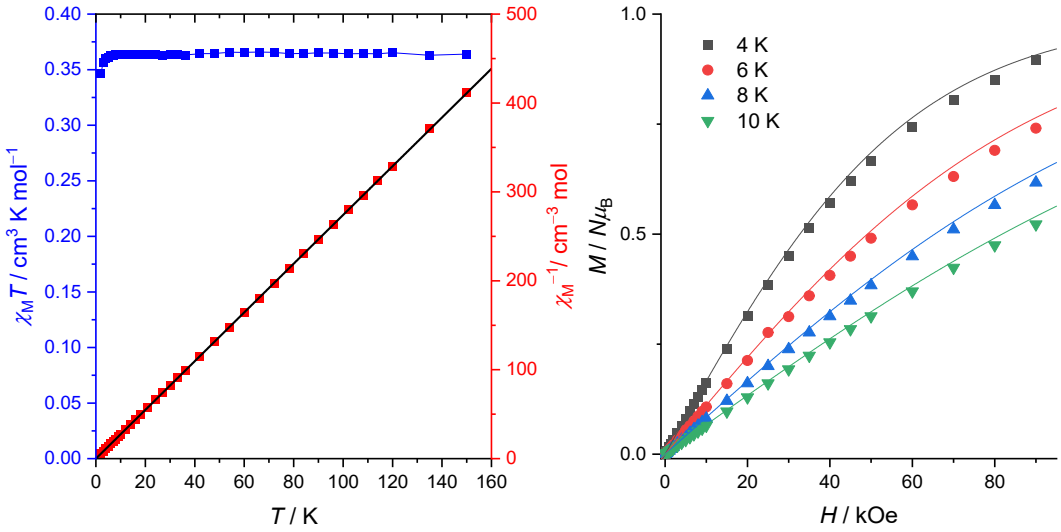

Figure S14. $\chi_M T$ vs. T plots at 10 kOe (left) and M vs. H plots (right) for **1m**. Solid line on χ_M^{-1} vs. T plots represents a fit in the T range of 20-100 K using Curie's law with a C value of 0.37 cm^3 K mol^{-1}. Brillouin function with S = 1/2 and g = 2 is shown as solid curves on M vs. H plots for comparison.

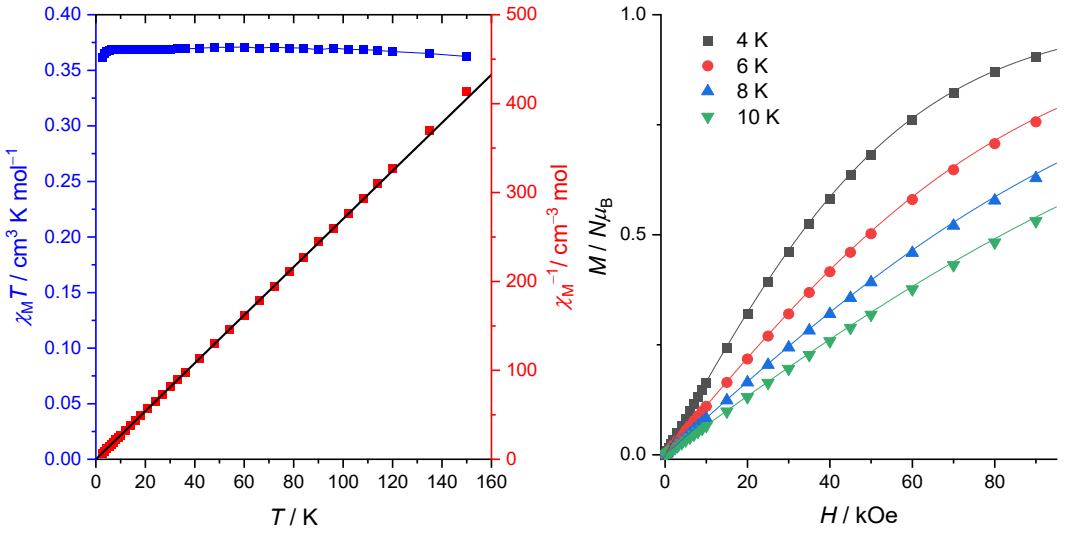

Figure S15. $\chi_M T$ vs. T plots at 10 kOe (left) and M vs. H plots (right) for **1g**. Solid line on χ_M^{-1} vs. T plots represent a fit in the T range of 20-100 K using Curie's law with a C value of 0.37 cm^3 K mol^{-1}. Brillouin function with S = 1/2 and g = 2 is shown as solid curves on M vs. H plots for comparison.

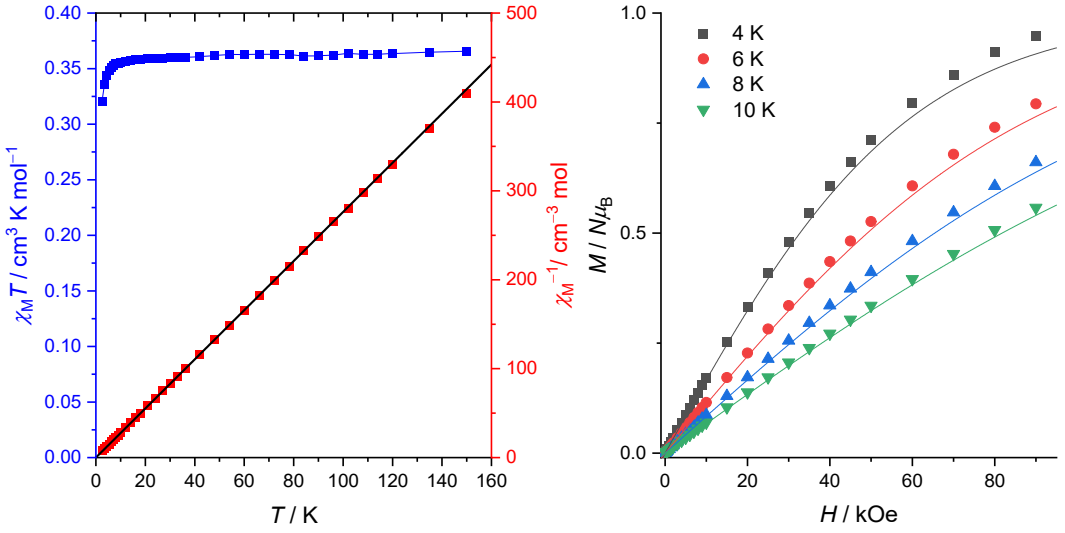

Figure S16. $\chi_M T$ vs. T plots at 10 kOe (left) and M vs. H plots (right) for **1s**. Solid line on χ_M^{-1} vs. T plots represents a fit in the T range of 20-100 K using Curie's law with a C value of 0.37 cm^3 K mol^{-1}. Brillouin function with S = 1/2 and g = 2 is shown as solid curves on M vs. H plots for comparison.

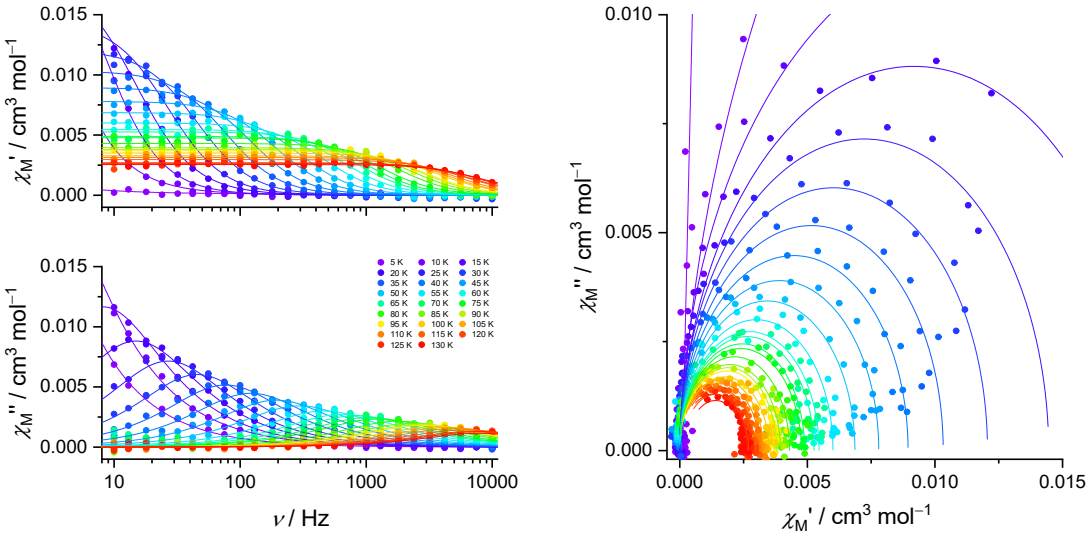

Figure S17. AC magnetic susceptibility of **1m** at a dc magnetic field of 10 kOe.

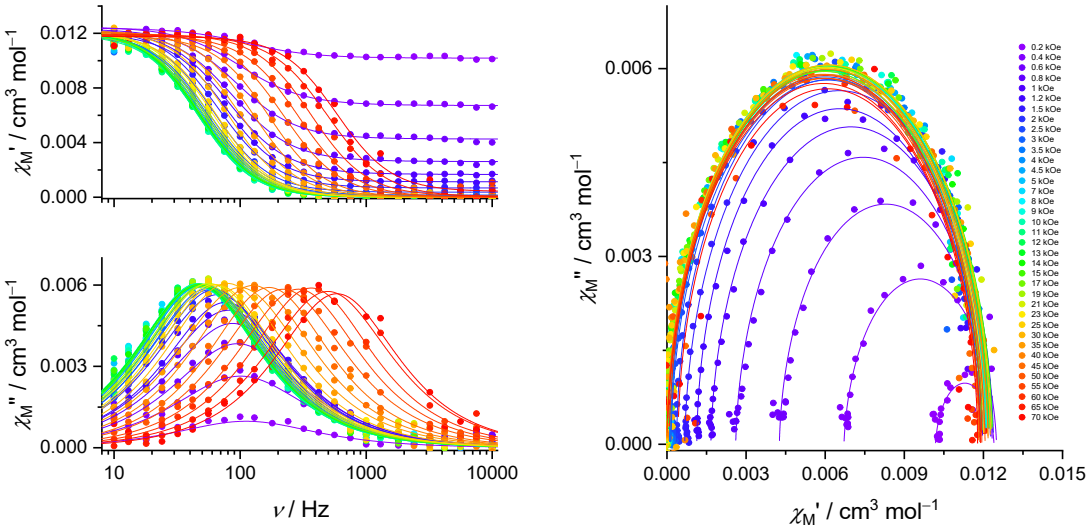

Figure S18. AC magnetic susceptibility of **1m** at 30 K.

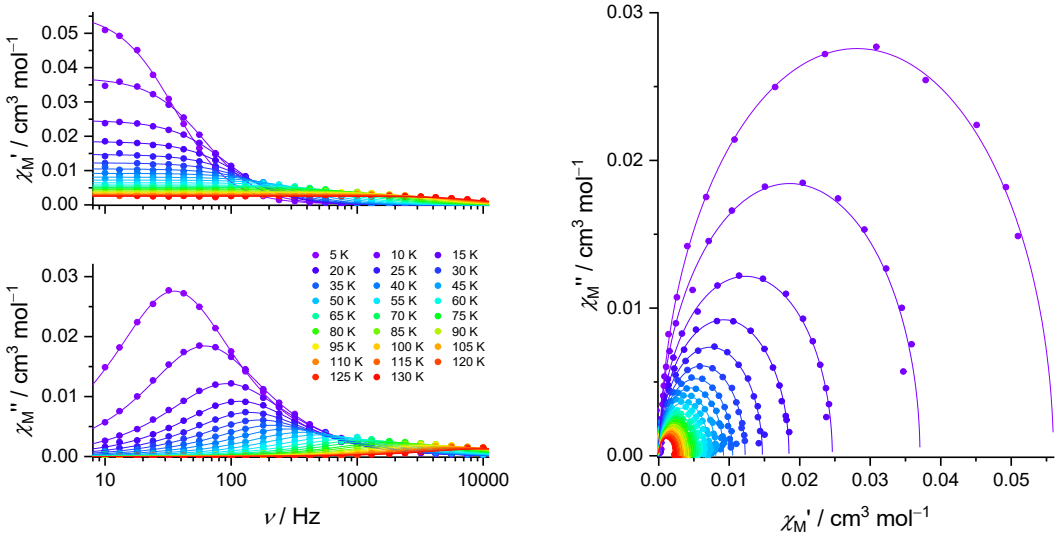

Figure S19. AC magnetic susceptibility of **1g** at a dc magnetic field of 10 kOe.

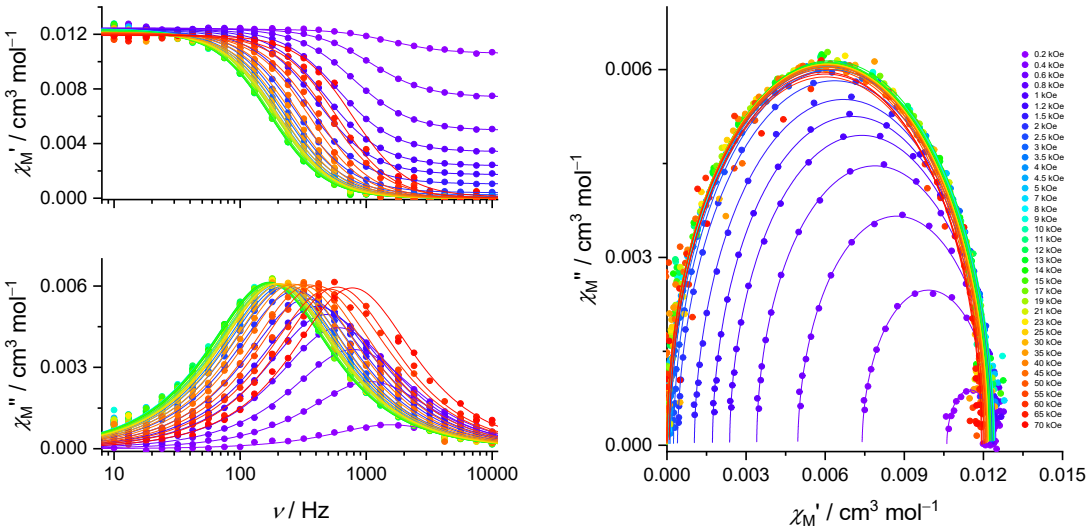

Figure S20. AC magnetic susceptibility of **1g** at 30 K.

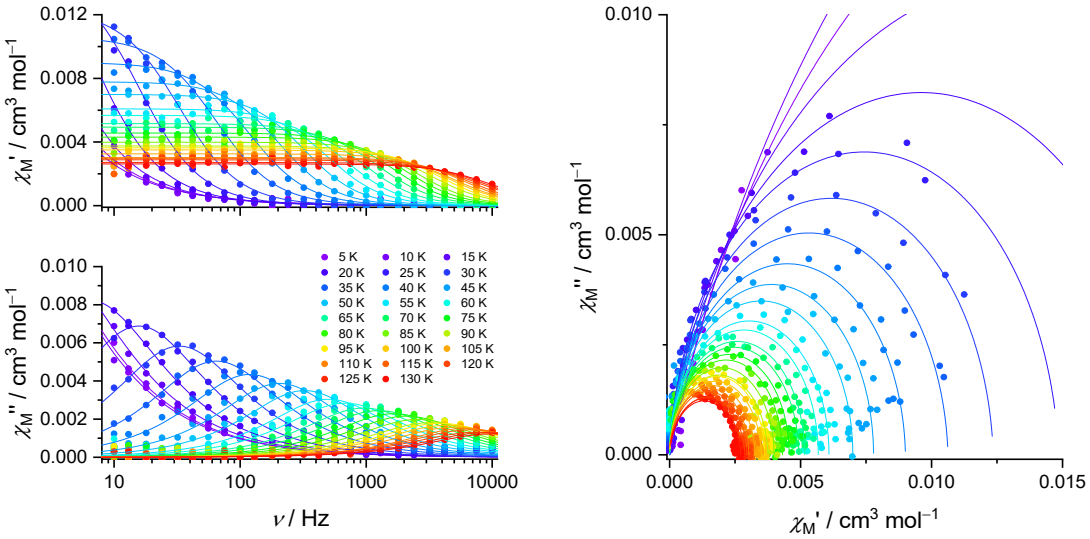

Figure S21. AC magnetic susceptibility of **1s** at a dc magnetic field of 10 kOe.

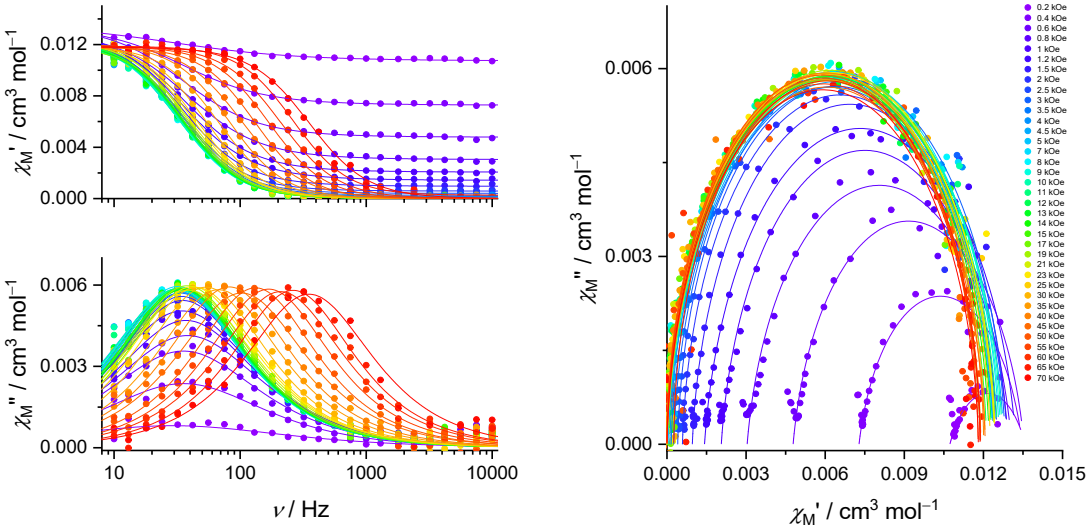

Figure S22. AC magnetic susceptibility of **1s** at 30 K.

Table S3. Parameters obtained by fitting the χ_M' and χ_M '' vs. ν plots of 1m at H = 10 kOe using generalized Debye model.

T / K	τ / μs	χ_S / cm^3 mol^{-1}	χ_T / cm^3 mol^{-1}	α
15	1.94(5) × 10^4	0	2.39(5) × 10^{-2}	0.03(2)
20	1.07(2) × 10^4	0	1.84(2) × 10^{-2}	0.03(1)
25	5.9(1) × 10^3	0	1.45(2) × 10^{-2}	0.03(1)
30	3.47(6) × 10^3	0	1.21(1) × 10^{-2}	0.01(1)
35	2.07(4) × 10^3	0	1.03(1) × 10^{-2}	0.02(1)
40	1.31(2) × 10^3	0	8.95(7) × 10^{-3}	0
45	8.2(2) × 10^2	0	7.80(8) × 10^{-3}	0.01(1)
50	5.4(1) × 10^2	0	6.86(6) × 10^{-3}	0
55	3.5(1) × 10^2	0	6.0(1) × 10^{-3}	0
60	2.4(1) × 10^2	0	5.46(9) × 10^{-3}	0.009(7)
65	1.9(1) × 10^2	0	5.3(1) × 10^{-3}	0.013(8)
70	1.5(1) × 10^2	0	4.9(1) × 10^{-3}	0.02(1)
75	1.27(5) × 10^2	0	4.78(6) × 10^{-3}	0
80	88(7)	0	4.30(8) × 10^{-3}	0.003(8)
85	69(5)	0	3.95(7) × 10^{-3}	0.014(9)
90	59(3)	0	3.80(5) × 10^{-3}	0
95	54(4)	0	3.69(5) × 10^{-3}	0
100	42(4)	0	3.37(6) × 10^{-3}	0.02(1)
105	36(2)	0	3.27(4) × 10^{-3}	0.012(9)
110	32(2)	0	3.14(4) × 10^{-3}	0.016(7)
115	26(2)	0	2.96(2) × 10^{-3}	0.01(1)
120	24(3)	1(3) × 10^{-4}	2.70(4) × 10^{-3}	0
125	20(2)	0	2.66(2) × 10^{-3}	0.02(1)
130	20(3)	3(2) × 10^{-4}	2.55(3) × 10^{-3}	0.01(1)

Fitting with generalized Debye model was performed with the constraint in that fitting parameters are greater than or equal to zero. Zero values on the table represent that fitting parameters adopt zero under this constraint.

Table S4. Parameters obtained by fitting the χ_M' and χ_M '' vs. ν plots of 1m at T = 30 K using generalized Debye model.

H / kOe	τ / μs	χ_S / cm^3 mol^{-1}	χ_T / cm^3 mol^{-1}	α
0.4	1.58(8) × 10^3	6.71(9) × 10^{-3}	1.25(1) × 10^{-2}	0.06(3)
0.6	1.67(5) × 10^3	4.26(7) × 10^{-3}	1.23(1) × 10^{-2}	0.03(2)
0.8	1.83(3) × 10^3	2.61(5) × 10^{-3}	1.23(1) × 10^{-2}	0.03(1)
1	1.97(2) × 10^3	1.67(3) × 10^{-3}	1.227(6) × 10^{-2}	0.03(1)
1.2	2.08(3) × 10^3	1.13(5) × 10^{-3}	1.197(9) × 10^{-2}	0.01(1)
1.5	2.38(4) × 10^3	6.7(5) × 10^{-4}	1.24(1) × 10^{-2}	0.02(1)
2	2.55(3) × 10^3	3.7(4) × 10^{-4}	1.203(8) × 10^{-2}	0
2.5	2.79(4) × 10^3	1.5(5) × 10^{-4}	1.20(1) × 10^{-2}	0.01(1)
3	2.87(5) × 10^3	1.4(5) × 10^{-4}	1.19(1) × 10^{-2}	0
3.5	3.00(3) × 10^3	1(3) × 10^{-4}	1.206(7) × 10^{-2}	0
4	3.18(4) × 10^3	0	1.221(9) × 10^{-2}	0.009(7)
4.5	3.25(4) × 10^3	0	1.22(1) × 10^{-2}	0.013(8)
5	3.37(6) × 10^3	0	1.21(1) × 10^{-2}	0.02(1)
7	3.45(6) × 10^3	0	1.22(1) × 10^{-2}	0
8	3.44(4) × 10^3	0	1.21(1) × 10^{-2}	0.003(8)
9	3.47(5) × 10^3	0	1.22(1) × 10^{-2}	0.014(9)
10	3.46(5) × 10^3	0	1.21(1) × 10^{-2}	0
11	3.39(4) × 10^3	0	1.19(1) × 10^{-2}	0
12	3.44(6) × 10^3	0	1.22(1) × 10^{-2}	0.02(1)
13	3.35(5) × 10^3	0	1.22(1) × 10^{-2}	0.012(9)
14	3.39(4) × 10^3	0	1.24(1) × 10^{-2}	0.016(7)
15	3.30(5) × 10^3	0	1.23(1) × 10^{-2}	0.01(1)
17	3.05(5) × 10^3	0	1.20(1) × 10^{-2}	0
19	3.01(6) × 10^3	0	1.23(2) × 10^{-2}	0.02(1)
21	2.82(5) × 10^3	0	1.23(1) × 10^{-2}	0.01(1)
23	2.59(3) × 10^3	0	1.205(9) × 10^{-2}	0
25	2.44(4) × 10^3	0	1.20(1) × 10^{-2}	0
30	2.01(4) × 10^3	0	1.23(1) × 10^{-2}	0.01(1)
35	1.59(4) × 10^3	0	1.22(2) × 10^{-2}	0.02(2)
40	1.26(3) × 10^3	0	1.22(1) × 10^{-2}	0.01(1)
45	9.4(3) × 10^2	0	1.18(2) × 10^{-2}	0
50	7.3(1) × 10^2	0	1.206(9) × 10^{-2}	0.02(1)
55	5.5(2) × 10^2	0	1.19(1) × 10^{-2}	0.01(2)
60	4.3(1) × 10^2	0	1.19(1) × 10^{-2}	0
65	3.20(9) × 10^2	0	1.189(9) × 10^{-2}	0.02(2)
70	2.7(1) × 10^2	0	1.18(1) × 10^{-2}	0

Fitting with generalized Debye model was performed with the constraint in that fitting parameters are greater than or equal to zero. Zero values on the table represent that fitting parameters adopt zero under this constraint.

Table S5. Parameters obtained by fitting the χ_M' and χ_M '' vs. ν plots of 1g at H = 10 kOe using generalized Debye model.

T / K	τ / μs	χ_S / cm^3 mol^{-1}	χ_T / cm^3 mol^{-1}	α
5	4.49(2) × 10^3	2.2(6) × 10^{-4}	5.6(2) × 10^{-2}	0.007(3)
10	2.57(2) × 10^3	9(8) × 10^{-5}	3.71(2) × 10^{-2}	0
15	1.720(8) × 10^3	0	2.463(7) × 10^{-2}	0
20	1.370(8) × 10^3	0	1.848(6) × 10^{-2}	0
25	1.140(9) × 10^3	0	1.471(6) × 10^{-2}	0
30	9.38(8) × 10^2	0	1.226(5) × 10^{-2}	0
35	7.4(1) × 10^2	0	1.05(6) × 10^{-2}	0
40	5.8(1) × 10^2	0	9.19(7) × 10^{-3}	0
45	4.25(6) × 10^2	0	8.09(5) × 10^{-3}	0
50	3.18(5) × 10^2	0	7.23(4) × 10^{-3}	0
55	2.38(7) × 10^2	0	6.45(6) × 10^{-3}	0
60	1.82(5) × 10^2	0	5.83(6) × 10^{-3}	0
65	1.39(4) × 10^2	0	5.45(5) × 10^{-3}	0
70	1.12(3) × 10^2	0	5.08(4) × 10^{-3}	0
75	88(3)	0	4.69(4) × 10^{-3}	0
80	72(2)	0	4.43(3) × 10^{-3}	0
85	59(2)	0	4.09(4) × 10^{-3}	0
90	50(2)	0	3.88(4) × 10^{-3}	0
95	42(2)	0	3.67(3) × 10^{-3}	0
100	36(2)	0	3.48(4) × 10^{-3}	0
105	31(2)	0	3.22(3) × 10^{-3}	0
110	27(1)	0	3.09(2) × 10^{-3}	0
115	24(1)	0	2.95(2) × 10^{-3}	0
120	20(2)	0	2.76(2) × 10^{-3}	0
125	18(2)	0	2.64(3) × 10^{-3}	0
130	16(3)	0	2.46(4) × 10^{-3}	0

Fitting with generalized Debye model was performed with the constraint in that fitting parameters are greater than or equal to zero. Zero values on the table represent that fitting parameters adopt zero under this constraint.

Table S6. Parameters obtained by fitting the χ_M' and χ_M'' vs. ν plots of 1g at T = 30 K using generalized Debye model.

H / kOe	τ / μs	χ_S / cm^3 mol^{-1}	χ_T / cm^3 mol^{-1}	α
0.4	1.48(4) × 10^2	7.40(7) × 10^{-3}	1.244(4) × 10^{-2}	0.01(2)
0.6	2.02(3) × 10^2	4.96(6) × 10^{-3}	1.247(4) × 10^{-2}	0.02(1)
0.8	2.64(4) × 10^2	3.40(6) × 10^{-3}	1.239(5) × 10^{-2}	0.004(10)
1	3.28(3) × 10^2	2.38(4) × 10^{-3}	1.240(3) × 10^{-2}	0.008(6)
1.2	3.89(3) × 10^2	1.72(4) × 10^{-3}	1.236(3) × 10^{-2}	0.008(5)
1.5	4.68(5) × 10^2	1.04(5) × 10^{-3}	1.235(5) × 10^{-2}	0.015(7)
2	5.75(6) × 10^2	4.0(5) × 10^{-4}	1.232(5) × 10^{-2}	0.015(6)
2.5	6.62(8) × 10^2	2.5(6) × 10^{-4}	1.233(6) × 10^{-2}	0.005(8)
3	7.17(6) × 10^2	1.2(4) × 10^{-5}	1.230(4) × 10^{-2}	0.01(5)
3.5	7.61(6) × 10^2	7(3) × 10^{-5}	1.228(4) × 10^{-2}	0.006(5)
4	8.0(1) × 10^2	3(6) × 10^{-5}	1.229(7) × 10^{-2}	0.008(8)
4.5	8.28(6) × 10^2	0	1.237(4) × 10^{-2}	0.01(5)
5	8.52(7) × 10^2	0	1.237(5) × 10^{-2}	0.013(6)
7	9.12(8) × 10^2	0	1.241(5) × 10^{-2}	0.013(5)
8	9.3(1) × 10^2	0	1.243(7) × 10^{-2}	0.014(8)
9	9.4(1) × 10^2	0	1.239(6) × 10^{-2}	0.011(7)
10	9.26(8) × 10^2	0	1.223(5) × 10^{-2}	0.001(5)
11	9.26(9) × 10^2	0	1.220(5) × 10^{-2}	0
12	9.35(8) × 10^2	0	1.224(5) × 10^{-2}	0
13	9.35(8) × 10^2	0	1.238(5) × 10^{-2}	0.005(6)
14	9.2(1) × 10^2	0	1.221(7) × 10^{-2}	0
15	9.29(9) × 10^2	0	1.229(5) × 10^{-2}	0.004(6)
17	8.87(9) × 10^2	0	1.217(6) × 10^{-2}	0
19	8.47(8) × 10^2	0	1.218(5) × 10^{-2}	0
21	8.3(1) × 10^2	0	1.215(7) × 10^{-2}	0
23	8.1(1) × 10^2	0	1.216(8) × 10^{-2}	0
25	7.9(1) × 10^2	0	1.218(7) × 10^{-2}	0
30	7.4(1) × 10^2	0	1.215(8) × 10^{-2}	0
35	6.7(2) × 10^2	0	1.21(1) × 10^{-2}	0
40	6.0(1) × 10^2	0	1.21(1) × 10^{-2}	0
45	5.3(1) × 10^2	0	1.212(9) × 10^{-2}	0
50	4.52(9) × 10^2	0	1.21(1) × 10^{-2}	0
55	3.9(1) × 10^2	0	1.20(1) × 10^{-2}	0
60	3.12(8) × 10^2	0	1.20(1) × 10^{-2}	0.01(2)
65	2.71(9) × 10^2	0	1.19(1) × 10^{-2}	0
70	2.05(4) × 10^2	0	1.195(7) × 10^{-2}	0

Fitting with generalized Debye model was performed with the constraint in that fitting parameters are greater than or equal to zero. Zero values on the table represent that fitting parameters adopt zero under this constraint.

Table S7. Parameters obtained by fitting the χ_M' and χ_M'' vs. ν plots of 1s at H = 10 kOe using generalized Debye model.

T / K	τ / μs	χ_S / cm^3 mol^{-1}	χ_T / cm^3 mol^{-1}	α
15	$6(1) \times 10^4$	0	$2.7(4) \times 10^{-2}$	0.15(2)
20	$2.4(2) \times 10^4$	0	$1.9(1) \times 10^{-2}$	0.10(2)
25	$1.0(3) \times 10^4$	0	$1.48(3) \times 10^{-2}$	0.05(1)
30	$4.8(1) \times 10^3$	0	$1.24(2) \times 10^{-2}$	0.04(1)
35	$2.46(5) \times 10^3$	0	$1.06(1) \times 10^{-2}$	0.03(1)
40	$1.34(3) \times 10^3$	0	$9.0(1) \times 10^{-3}$	0.02(1)
45	$7.8(2) \times 10^2$	0	$7.79(8) \times 10^{-3}$	0
50	$4.8(2) \times 10^2$	0	$6.9(1) \times 10^{-3}$	0
55	$3.2(1) \times 10^2$	0	$6.1(1) \times 10^{-3}$	0
60	$2.3(1) \times 10^2$	0	$5.67(9) \times 10^{-3}$	0
65	$1.66(7) \times 10^2$	0	$5.16(7) \times 10^{-3}$	0
70	$1.26(6) \times 10^2$	0	$4.93(7) \times 10^{-3}$	0
75	95(5)	0	$4.57(7) \times 10^{-3}$	0
80	76(4)	0	$4.31(6) \times 10^{-3}$	0
85	61(5)	0	$4.02(8) \times 10^{-3}$	0
90	49(4)	0	$3.75(7) \times 10^{-3}$	0
95	40(4)	0	$3.59(7) \times 10^{-3}$	0
100	36(4)	0	$3.42(6) \times 10^{-3}$	0
105	32(3)	0	$3.26(4) \times 10^{-3}$	0
110	36(4)	0	$3.02(6) \times 10^{-3}$	0
115	23(4)	0	$2.94(5) \times 10^{-3}$	0
120	20(6)	0	$2.76(7) \times 10^{-3}$	0
125	17(7)	0	$2.59(8) \times 10^{-3}$	0
130	16(3)	0	$2.59(3) \times 10^{-3}$	0

Fitting with generalized Debye model was performed with the constraint in that fitting parameters are greater than or equal to zero. Zero values on the table represent that fitting parameters adopt zero under this constraint.

Table S8. Parameters obtained by fitting the χ_M' and χ_M '' vs. ν plots of 1s at T = 30 K using generalized Debye model.

H / kOe	τ / μs	χ_S / cm^3 mol^{-1}	χ_T / cm^3 mol^{-1}	α
0.4	4.5(3) × 10^3	7.3(7) × 10^{-3}	1.45(2) × 10^{-2}	0.17(3)
0.6	4.5(2) × 10^3	4.8(6) × 10^{-3}	1.35(2) × 10^{-2}	0.13(2)
0.8	4.2(2) × 10^3	3.0(7) × 10^{-3}	1.31(2) × 10^{-2}	0.12(2)
1	4.3(1) × 10^3	2.1(5) × 10^{-3}	1.29(2) × 10^{-2}	0.09(1)
1.2	4.6(1) × 10^3	1.4(5) × 10^{-3}	1.32(2) × 10^{-2}	0.10(1)
1.5	4.54(9) × 10^3	9.6(4) × 10^{-4}	1.29(1) × 10^{-2}	0.06(1)
2	4.6(1) × 10^3	5.9(6) × 10^{-4}	1.25(2) × 10^{-2}	0.04(1)
2.5	4.59(7) × 10^3	4.1(4) × 10^{-4}	1.24(1) × 10^{-2}	0.029(8)
3	4.93(8) × 10^3	2.5(4) × 10^{-4}	1.28(1) × 10^{-2}	0.045(9)
3.5	4.76(7) × 10^3	1.6(4) × 10^{-4}	1.24(1) × 10^{-2}	0.043(8)
4	4.83(9) × 10^3	1.1(5) × 10^{-4}	1.25(1) × 10^{-2}	0.04(1)
4.5	5.1(1) × 10^3	0	1.28(2) × 10^{-2}	0.06(1)
5	4.83(8) × 10^3	0	1.24(1) × 10^{-2}	0.031(9)
7	4.95(8) × 10^3	0	1.26(1) × 10^{-2}	0.037(9)
8	4.9(1) × 10^3	0	1.23(2) × 10^{-2}	0.04(1)
9	5.04(9) × 10^3	0	1.27(1) × 10^{-2}	0.05(1)
10	5.1(1) × 10^3	0	1.27(2) × 10^{-2}	0.06(1)
11	4.8(1) × 10^3	0	1.26(2) × 10^{-2}	0.04(1)
12	4.62(9) × 10^3	0	1.21(2) × 10^{-2}	0.02(1)
13	4.63(8) × 10^3	0	1.23(1) × 10^{-2}	0.03(1)
14	4.51(9) × 10^3	0	1.22(2) × 10^{-2}	0.03(1)
15	4.59(9) × 10^3	0	1.25(2) × 10^{-2}	0.04(1)
17	4.15(9) × 10^3	0	1.19(2) × 10^{-2}	0.01(1)
19	4.20(7) × 10^3	0	1.24(1) × 10^{-2}	0.02(1)
21	4.08(9) × 10^3	0	1.24(2) × 10^{-2}	0.04(1)
23	3.82(8) × 10^3	0	1.25(2) × 10^{-2}	0.03(1)
25	3.54(7) × 10^3	0	1.23(2) × 10^{-2}	0.02(1)
30	2.97(6) × 10^3	0	1.21(2) × 10^{-2}	0.01(1)
35	2.36(5) × 10^3	0	1.19(2) × 10^{-2}	0.01(1)
40	1.94(3) × 10^3	0	1.20(1) × 10^{-2}	0
45	1.55(4) × 10^3	0	1.21(1) × 10^{-2}	0.04(1)
50	1.20(2) × 10^3	0	1.18(1) × 10^{-2}	0
55	9.4(2) × 10^2	0	1.19(1) × 10^{-2}	0
60	7.6(2) × 10^2	0	1.19(1) × 10^{-2}	0.02(2)
65	6.1(2) × 10^2	0	1.19(1) × 10^{-2}	0
70	4.5(1) × 10^2	0	1.18(1) × 10^{-2}	0.03(2)

Fitting with generalized Debye model was performed with the constraint in that fitting parameters are greater than or equal to zero. Zero values on the table represent that fitting parameters adopt zero under this constraint.